Spectrometry behind concrete shielding for neutrons produced by 400 MeV/u ^{12}C ions impinging on a thick graphite target

Georg Fehrenbacher[1], Burkhard Wiegel[2], Hiroshi Iwase[1], Torsten Radon[1], Dieter Schardt[1], Helmut Schuhmacher[2] and Jürgen Wittstock[2]

[1]GSI - Gesellschaft für Schwerionenforschung, Planckstr. 1, 64291 Darmstadt, Germany
E-mail: g.fehrenbacher@gsi.de
[2]Physikalisch-Technische Bundesanstalt, Bundesallee 100, 38116 Braunschweig, Germany

Abstract. Neutron spectra were measured at the GSI heavy ion accelerator using the Bonner sphere spectrometer NEMUS. The irradiation experiments were carried out at Cave A, an experimental area at the GSI heavy ion synchrotron SIS. A 400 MeV/u carbon ion beam impinging on a thick graphite target was used as neutron source. Spectral distributions were determined by unfolding the measured readings using the unfolding code MAXED for four positions outside the shielding and for four positions in the entry maze of Cave A. First results are presented for two positions from Monte Carlo simulations carried out with a newer version of FLUKA considering both the particle production in nucleus-nucleus collisions and the transportation of particles through the shielding. Measured and calculated neutron spectra are compared for these positions.

1. Introduction

Heavy ion accelerators are mainly used for research in physics hitherto. Meanwhile heavy ions are passing into broader applications like the treatment of tumour patients in dedicated clinical facilities. The radiation protection for the operation of heavy ion accelerators with ion energies at a few hundred MeV per nucleon (MeV/u) to a few GeV per nucleon (GeV/u) deals mainly with the shielding of the produced neutron radiation. The neutron radiation is generated when the heavy ion beam interacts with the nuclei of the accelerator components during the transportation to experimental areas. Within the experimental areas neutron radiation is mainly produced in the target or in the beam stop.

For the operation of heavy ion accelerators improvements are needed in the knowledge of neutron radiation fields. Double differential distributions (energy and angle) of the neutron radiation originating from 400 MeV/u carbon beams stopped in a thick graphite target were measured by Kurosawa et al. [1]. In the work of Gunzert-Marx [2] double differential neutron distributions were measured for thick water and graphite targets irradiated by 200 MeV/u and 400 MeV/u carbon beams, respectively. For heavy ion beams in this energy range measurements of neutron spectra outside shielding are scarce. Knowledge of these neutron spectra is necessary for the shielding design of accelerators and experimental areas or the calibration of dosemeters (personal dosemeters as well as area monitors).

Subject of this work is the measurement of neutron spectra outside the shielding of an experimental area at GSI. For this investigation the experimental area at Cave A at the heavy ion synchrotron (SIS) was chosen. A 400 MeV/u carbon beam, stopped in a thick graphite target, was used as a neutron source. The measurement positions were laterally and in forward direction to the target position and along the entry maze of Cave A (see Fig. 1).

The neutron measurements were carried out with the **Ne**utron **Mu**ltisphere **S**pectrometer NEMUS developed at PTB [3]. The spectral neutron fluence distributions are derived by unfolding the readings of the detectors in the spheres. The results for two measurement positions (OC-11, 13) are compared with computed neutron distributions. For the computations a new version of the MC (Monte Carlo) code FLUKA [4] was used where nucleus-nucleus collisions are considered. For the MC calculations a geometrical model of Cave A was developed in order to achieve a realistic simulation of the neutron radiation fields inside and outside the cave.
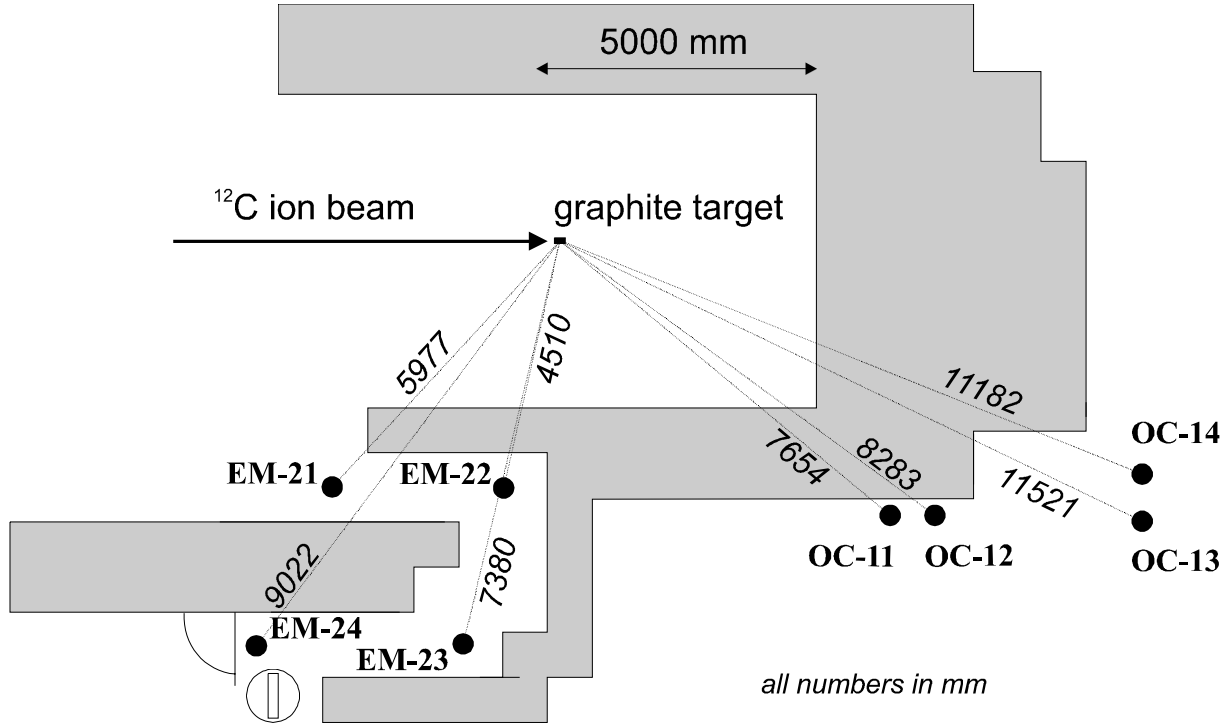
FIG. 1. Scheme of the irradiation geometry for the measurements of neutron spectra caused by ^{12}C ions stopped in a graphite target. The measurements were performed at the positions OC-11, 12, 13 and 14 outside the concrete shielding and along the entry maze at the positions EM-21, 22, 23 and 24. The impinging carbon ion beam had an energy of 400 MeV per nucleon.

The measurements give an impression on neutron spectra to be expected outside the concrete shielding at heavy ion accelerators, the comparison with the results of the new version of FLUKA gives a first idea on the reliability of the used models for the neutron production in nucleus-nucleus collisions in combination with the subsequent neutron transport in the concrete shielding.

2. Ion beam characteristics and beam monitoring

Carbon ion beams were produced in an ECR (electron cyclotron resonance) source, pre-accelerated in the UNILAC (Universal Linear Accelerator) to about 8 MeV per nucleon and subsequently injected in the heavy ion synchrotron SIS. In the SIS the carbon ions were accelerated to the energies of request, here 400 MeV/u. The accelerated ions circulating in the synchrotron were extracted by the electrical field of a septum wire (slow extraction). The slow extraction method should prevent pile-up effects in the counters of NEMUS. The total period for the extraction was about 1 s and the repetition cycle was one pulse every 2.9 s. The average beam intensity was 10^8 to 10^9 ions in one beam pulse.

At the end of the beam line the primary pencil-like carbon beam passed through a secondary electron transmission monitor (SEETRAM) [6] and a thin vacuum exit window (aluminium, 100 μm thick). Behind the window the beam was stopped in a 20 cm thick graphite target ($\rho = 1.8$ g·cm^{-3}) with a quadratic cross section of 10×10 cm^2 perpendicular to the beam axis. The calculated mean range of the carbon ions in the target is 13.3 cm [7]. The SEETRAM consists of three thin titanium foils (each 10 μm thick). Secondary electrons produced by the beam particles are collected by applying a voltage of 80 V between the middle foil and the two outer foils. The current was recorded and integrated by a high-accuracy electrometer and read-out at the end of each beam pulse. The SEETRAM offers the advantage of good linearity at high beam currents. It was calibrated by simultaneous measurements with a parallel-plate ionization chamber at lower beam currents.

3. Measurements and Unfolding

3.1. The neutron spectrometer

For the neutron spectrum measurements the **N**eutron **Mu**ltisphere **S**pectrometer NEMUS was used [3]. The NEMUS is an extended Bonner sphere spectrometer and consists of ten polyethylene spheres with diameters from 7.62 cm (3") to 30.48 cm (12"), a bare and a cadmium shielded bare detector and in addition four spheres made of polyethylene with copper or lead inlets. All units contain a ³He-filled spherical proportional counter (type SP-9, Centronic Ltd., UK) used as a central thermal-neutron-sensitive detector. The spheres with an additional metal inlet have an improved response to high energy neutrons due to (n, xn) reactions.

3.2. Selection of measurement positions

Two general areas, *OC* and *EM*, were selected to determine the neutron spectra (see Fig. 1). In the area *OC* (outside Cave A) the measurement positions were OC-11, 12, 13, 14 and in area *EM* (entry maze of Cave A) the four positions were EM-21, 22, 23, 24. The 14 spheres of NEMUS could not be placed simultaneously at these positions to avoid a mutual disturbance of the neutron field. Therefore four different spheres were irradiated at four OC positions at once (typical measurement period was 10 to 20 min.). During the next period the spheres were exchanged and then replaced by further spheres of the NEMUS set until at least ten spheres were irradiated at each position. For the measurements in the entry maze only two positions were measured at the same time: EM-21, 22 and at last EM-23, 24. Especially the measurements outside the cave (OC positions) were interrupted by many hours due to higher priority of other experiments. All following results are only valid under the assumption that the neutron field, i.e. at least the spectrum shape, did not change during the whole campaign. For the later analysis of the experiment it was necessary to have a precise monitoring of the primary carbon beam (see beam monitoring).

3.3. Spectrum determination with MAXED

The spectral neutron fluence distribution must be derived by unfolding the readings M_d of the detectors inside the spheres labelled by their diameter d. This mathematical deconvolution was done by application of the computer code MAXED [8, 9]. The following equation must be solved for the neutron fluence distribution $\Phi_E(E_n)$:

$$M_d = \int R_d(E_n)\Phi_E(E_n)dE_n \tag{1}$$

with the response $R_d(E_n)$ of the sphere with diameter d at the neutron energy E_n. Details of the algorithm and the mathematical background of unfolding can be found in Ref. [8, 9]. Basis of the unfolding are the response functions of the detection units in the entire neutron energy range to be expected. The response functions $R_d(E_n)$ were computed by means of the MC code MCNPX [10]. A detailed description of the geometry model and results are published in Ref. [3].

4. Computation of Spectral Neutron Fluence Distributions with FLUKA

In 2003 a new version of the FLUKA code (version 2003.1) was released which enables the simulation of heavy ion transport including nucleus-nucleus interactions [11]. For the high energy part (E > 5 GeV/u) the DPMJET code was installed into FLUKA. For the lower energy range of heavy ions (100 MeV/u < E < 5 GeV/u) the RQMD (Relativistic Quantum Molecular Dynamic) model was incorporated. In the transport simulation below 100 MeV/u the heavy ions undergo no inelastic collisions but are slowed down to rest. The transportation of neutrons is particular based on a multi-group cross section library with 72 energy groups from 1.0E–5 eV to 19.6 MeV. For higher neutron energies the neutron transport is performed in a fully analogue mode. A geometrical model for Cave A was developed for the transport of the secondary radiation.

Table I. For the shielding calculations the following element composition for the concrete shielding was assumed. The density is considered with a value of 2.35 g/cm^3.

Element	H	C	O	Na	Al	Fe	Si	Ca
Fraction of mass (%)	0.6	0.4	51.1	0.3	2.0	1.2	35.8	8.6

The components of the concrete were assumed as the element composition given in Table I. Due to the thick concrete shielding of Cave A (1.6 m lateral and 4.8 m forward) the calculations were time-consuming and took about 3.5 days. The computations were carried out at the GSI Linux cluster using 100 processors.

5. Results and Discussion

5.1. Criteria for the default spectrum

For the unfolding procedure some *a priori* information is necessary which is included in so-called default spectra. In the cases of the outside positions the knowledge of similar neutron radiation fields were used. From previous experiments with high energy neutrons passing through massive shielding, for example the thick concrete walls at the CERN high-energy reference field CERF [12, 13] or the total thickness of the atmosphere at sea level [14] one expects a peak at about 100 MeV. The total neutron cross sections of the elements present in the shielding material show a minimum at this energy [15]. A second peak is expected around 1 MeV which arises from evaporation reactions. At thermal energies a small peak is most probable and in the intermediate region a $1/E^\alpha$ shape is assumed. Several default spectra with different portions of fluence within the above mentioned energy regions were tested. But all different default spectra lead to very similar final (result) spectra, i.e. the relative height of the peaks has only a very minor influence on the result as long as one starts with this general shape.
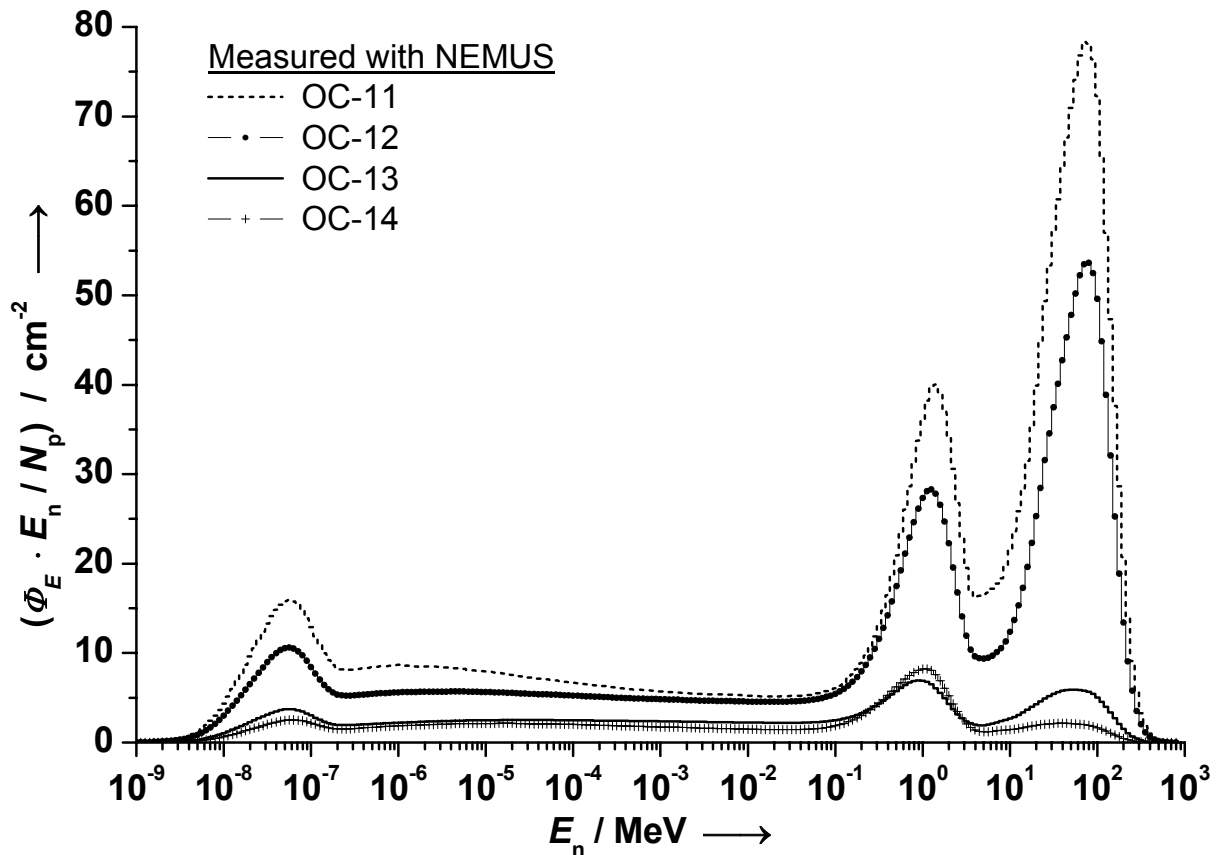

FIG. 2. Neutron spectra measured with the NEMUS system, unfolded with MAXED [8], for a 400 MeV/u ^{12}C ion beam impinging on a thick graphite target. The labels OC-11, 12, 13, 14 correspond to the measurement positions outside cave A (see also Fig. 1). The spectra are presented in a lethargy plot per $N_p = 10^{10}$ ions.

5.2. Neutron spectra outside Cave A

The results for the measurement points outside Cave A are given in Fig. 2 for the positions OC-11, 12, 13, 14. Although the neutron production yield is lowered with increasing angle the total height of the neutron spectra is dominated by the spectrum at position OC-11. This is due to the circumstance that OC-11 has the closest distance to the target and the attenuation thickness in the concrete shielding is the lowest.

The ratio of the two peaks at 1 MeV and 100 MeV is mainly determined by the element composition of the shielding material, the attenuation length of the radiation in the shielding (line of sight) and the primary neutron spectrum, which is a function of the angle relative to the beam line.

5.3. Neutron spectra in the entry maze

The situation is different for the measurements in the entry maze. Here in the line of sight from the measurements points to the target one has only a contribution of source neutrons with an angle of 90° or larger. This implies that the mean neutron energy is substantially lower than in forward direction (see also the primary neutron spectrum of Kurosawa et al. [1]). Due to the geometry of the entry maze a higher proportion of scattered neutron radiation is expected. In Fig. 3 one can see that in addition to the 1 MeV and 100 MeV peak a high contribution to the neutron spectrum comes from the scattered neutrons with a peak at 0.05 eV. The neutron scattering is caused not only by the walls in the cave and in the maze, but also by the internals in the cave. With an increasing distance from the target to the measurement points (EM-21, 22, 23, 24 increasing path length in the maze) the proportion of the low energy peak at 0.05 eV rises.
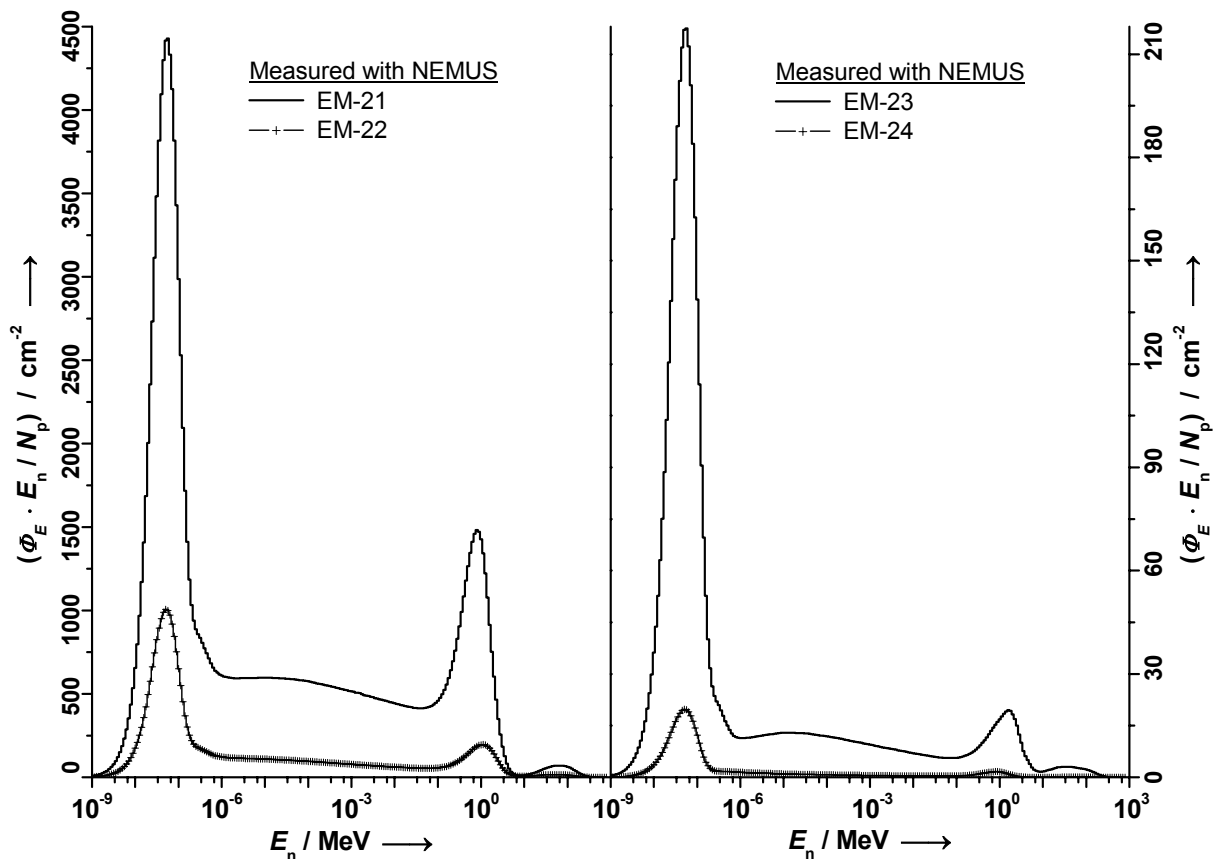

FIG. 3. *Measured neutron spectra, unfolded with MAXED, in the entry maze for ^{12}C ions with 400 MeV/u impinging on a thick graphite target. The spectra are presented in a lethargy plot per $N_p = 10^{10}$ ions.*

It can also be observed that the 100 MeV peak in comparison to the 1 MeV peak is damped if the angle to the ion beam line is enlarged or if the attenuation length in the shielding is increased (see also Fig. 2). There can be two reasons mentioned for this effect. The first one is that the source neutron spectrum has a lower proportion of high energy neutrons with an increasing angle. The second one is the fact that the high energy neutrons are involved in elastic and inelastic scattering processes (evaporation) where instantly neutrons in the MeV range are produced or neutrons with lower energies are released.

5.4. Comparison of measured and calculated spectra

For one lateral and one forward measurement position (OC-11, 13) neutron spectra were computed by means of the MC code FLUKA. First results for the comparison of the measured and calculated distributions are given in Fig. 4. At position OC-11 the FLUKA calculations result in a more structured distribution with a third peak at about 5 MeV, which was not confirmed by the MAXED unfolding when the FLUKA spectrum was used as a guess spectrum. In the FLUKA calculations the height of the 1 MeV and 100 MeV peak are approximately the same, in contrast the measurement gives a higher 100 MeV peak compared to the 1 MeV peak. For position OC-13 both distributions are rather similar. The statistical (type A) uncertainty of the calculated fluence per energy bin is approximately 5-20% for OC-11 and 10-30 % for the OC-13 position.
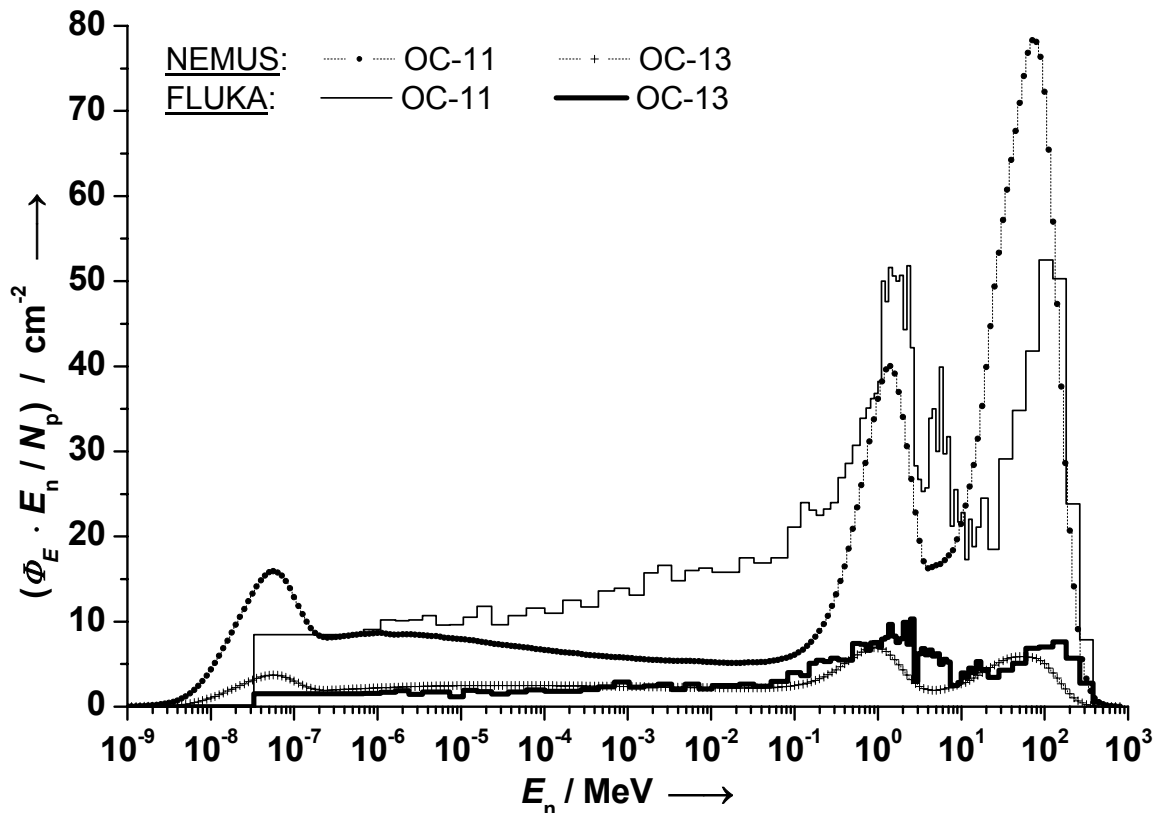

FIG. 4. Absolute comparison of measured (NEMUS) and calculated (FLUKA) neutron spectra at two positions outside the cave for ^{12}C ions with 400 MeV/u impinging on a thick graphite target. The spectra are presented in a lethargy plot per $N_p = 10^{10}$ ions.

Due to the multi-group neutron cross section used in FLUKA it is not possible to calculate the neutron spectrum at low energies with a high resolution. A neutron transport cut-off at 0.4 eV was applied to save computing time and consequently no neutrons below 0.4 eV were considered. A comparison of calculated and measured total neutron fluence (in the energy interval 0.4 eV < E_n < 1000 MeV) shows that the FLUKA calculations overestimate the NEMUS measurements by approximately 20% for the two positions shown in Fig. 4. The relative standard uncertainty of the measured fluence is estimated to be 7%. This includes the type A (statistical) uncertainties of the detector readings M_d (which is the

smallest contribution with less than 1.5%), the type B (systematic) uncertainties due to the choice of the default spectrum and the uncertainties of the Bonner sphere response functions. A detailed analysis of the uncertainty budget for NEMUS is under development. The uncertainty of the monitoring system is not taken into account. For the FLUKA calculations only type A (statistical) uncertainties are known which are less than 1.5%.

6. Summary and Conclusion

In this work spectrometric neutron measurements have been performed. For the measurements a shielded experimental area at GSI (Cave A) was used, where a 400 MeV/u carbon beam impinged on a thick graphite target providing high-fluence neutron fields. The neutron spectrum measurements, carried out with the extended Bonner sphere spectrometer NEMUS [3], were performed outside the concrete shielding in forward and lateral direction (4 positions) and in the entry maze of the cave (4 positions). The unfolding of the measured readings was done by means of the unfolding code MAXED [8].

The results of the unfolding show for the measurement positions in forward and lateral direction pronounced peaks at 1 MeV and 100 MeV which agrees with previous measurements at accelerators [13]. This is due to the fact that high energetic neutrons cause evaporation reactions with the emission of neutrons in the MeV range by excited nuclei and the reduced cross sections for (inelastic) scattering of neutrons in the 100 MeV range for the elements to be considered for the shielding materials. For the measurements in the entry maze a third peak in the neutron spectrum at 0.05 eV was observed whilst the other two peaks are damped.

First calculations were carried out with the MC code FLUKA which was recently extended by heavy ion transport considering the nucleus-nucleus collisions down to 100 MeV/u. A comparison was done for the neutron spectra for one lateral and forward position. The structure of the computed spectra is similar to the measured ones. The computed spectrum in lateral position shows an additional peak at 5 MeV, but no peak for the thermal neutrons.

In general it can be stated that the computed neutron spectra agree roughly within a factor of two to the measured ones. Further work is necessary to understand the deviations.

7. References

1. Kurosawa T., Nakao N., Nakamura T., Uwamino Y., Shibata T., Nakanishi N., Fukumura A., and Murakami K., *Measurements of secondary neutrons produced from thick targets bombarded by high-energy helium and carbon ions*, Nucl. Sci. Eng., 132:30-56 (1999).
2. Gunzert-Marx K., *Nachweis leichter Fragmente aus Schwerionenreaktionen mit einem BaF$_2$-Teleskop-Detektor, Messungen im Rahmen des Tumortherapieprojekts der GSI,* PHD-thesis, Technical University of Darmstadt (2004) (in German).
3. Wiegel B., Alevra A.V., *NEMUS – the PTB Neutron Multisphere Spectrometer: Bonner Spheres and more*, Nucl. Instr. Meth. Phys. Res. A 476: 36-41 (2002).
4. Fassò A., Ferrari A., Sala P.R., *Electron-photon transport in FLUKA: Status*, Proceedings of the Monte Carlo 2000 Conference, Lisbon, 23-26 October 2000, edited by A. Kling, F. Barao, M. Nakagawa, L. Tavora, P. Vaz, (Springer-Verlag Berlin, 2001), pp. 159-164.
5. Fassò A., Ferrari A., Ranft J., Sala P.R., *FLUKA: Status and prospective for hadronic applications*, Proceedings of the Monte Carlo 2000 Conference, Lisbon, 23-26 October 2000, edited by A. Kling, F. Barao, M. Nakagawa, L. Tavora, P. Vaz, (Springer-Verlag Berlin, 2001), pp. 955-960.
6. Jurado, B., Schmidt, K.-H., Behr K.-H., *Application of a secondary-electron transmission monitor for high-precision intensity measurements of relativistic heavy-ion beams*, Nucl. Instrum. Meth. in Phys. Res. A 483:603-610 (2002).
7. Geissel H., Scheidenberger C., *Slowing down of relativistic heavy ions and new applications,* Nucl. Instrum. Meth. in Phys. Res. B 136-138: 114-124 (1998).
8. Reginatto M. and Goldhagen P., *MAXED, a computer code for maximum entropy deconvolution of multisphere neutron spectrometer data*. Health Phys. 77:579-583 (1999).

9. Reginatto R., Goldhagen P., Neumann S., *Spectrum unfolding, sensitivity analysis and propagation of uncertainties with the maximum entropy deconvolution code MAXED*, Nucl. Instr. Meth. Phys. Res. A 476: 242-246 (2002).

10. Briesmeister J.F. (Ed.), *MCNP – A General Monte Carlo N-Particle Transport Code, Version 4B*, Manual LA-12625-M, March 1997
and
Waters L.S. (Ed.), *MCNPX User's Manual, Version 2.1.5*, TPO-E83-G-UG-X-00001, Rev. 0, November 1999.

11. Fassò A., Ferrari A., Roesler S., Sala P.R., Ballarini F., Ottolenghi A., Battistoni G., Cerutti F., Gadioli E., Garzelli M.V., Empl A., Ranft J., in Proceedings of the Conference on Computation in High Energy and Nuclear Physics (Chep03-MOMT005) La Jolla, California, March 24 - 28, 2003, *The physics models of FLUKA: Status and recent developments*, ePrint Archive: hep-ph/0306267 (2003).

12. Birattari C., Ferrari A., Höfert M., Otto T., Rancati T., Silari M., *Recent results at the CERN-EC High Energy Reference Field Facility*. In: "Third Specialists Meeting on Shielding Aspects of Accelerators, Targets and Irradiation Facilities (SATIF-3) at Tohoku University, Sendai, Japan". edited by OECD (1998), p. 219-234.

13. Höfert M., Stevenson G.R., *The CERN-CEC High Energy Reference Field Facility*. in Proceedings of the 8th International Conference on Radiation Shielding at Arlington, Texas, USA (American Nuclear Society, Inc., Illinois, USA, 1994), p. 635-642.

14. Wiegel B. et al., *Spectrometry with the PTB Neutron Multisphere Spectrometer (NEMUS) at Flight Altitudes and at Ground Level*. Nucl. Instrum. Meth. A476: 52-57 (2002).

15. Abfalterer W. P. et al*., Measurement of neutron total cross sections up to 560 MeV*, Phys. Rev. C 63:044608, 19 pages (2001).